Poly(vinyl pyrrolidone-*co*-octavinyl polyhedral oligomeric silsesquioxane) Hybrid Nanocomposites: Preparation, Thermal Properties, and T_g Improvement Mechanism

Benhong Yang,[1,2] Jirong Li,[1,3] Jiafeng Wang,[3] Hongyao Xu,[1,3] Shangyi Guang,[1] Cun Li[3]

[1]*College of Material Science and Engineering & State Key Laboratory for Modification of Chemical Fibers and Polymeric Materials, Donghua University, Shanghai 201620, China*
[2]*Department of Chemistry and Material Engineering, Hefei University, Hefei 230022, China*
[3]*School of Chemistry and Chemical Engineering, Anhui University, Hefei 230039, China*

Received 24 August 2008; accepted 4 September 2008
DOI 10.1002/app.29321
Published online 5 December 2008 in Wiley InterScience (www.interscience.wiley.com).

ABSTRACT: A series of poly(vinyl pyrrolidone-*co*-octavinyl polyhedral oligomeric silsesquioxanes) (PVP-POSS) organic–inorganic hybrid nanocomposites containing different percentages of POSS were prepared via free radical polymerization and characterized by FTIR, high-resolution ^{1}H-NMR, solid-state ^{29}Si-NMR, GPC, DSC, and TGA. POSS contents in these nanocomposites can be effectively controlled by varying the POSS feed ratios which can be accurately quantified by FTIR curve calibration. On the basis of ^{29}Si-NMR spectra, average numbers of reacted vinyl groups of each octavinyl-POSS macromer are calculated to be 5–7, which depends on POSS feed ratios. Both GPC and DSC results indicate that these nanocomposites display network structure and the degree of crosslinking increases with the increase of the POSS content. The incorporation of POSS into PVP significantly improves their thermal properties (T_g and T_{dec}) primarily due to crosslinking structure and dipole–dipole interaction between POSS cores and PVP carbonyl groups. © 2008 Wiley Periodicals, Inc. J Appl Polym Sci 111: 2963–2969, 2009

Key words: nanocomposites; polyvinyl pyrrolidone; free radical polymerization; thermal properties; polyhedral oligomeric silsesquioxane

INTRODUCTION

Organic–inorganic nanocomposites have attracted much attention because they may combine the advantages of both traditional organic polymers (e.g., processability and toughness) and inorganic materials (e.g., rigidity and stability). Polyhedral oligomeric silsesquioxanes (POSS) with cubic structure are a type of special molecules. Their corners are often connected to organic functional groups, which impart POSS excellent ability to copolymerize with other organic monomers, forming organic–inorganic hybrid nanocomposites with a variety of structures such as linear,[1–11] star-shaped[12–15] as well as network types.[16–29] In these hybrid nanocomposites, the inorganic nanosize POSS moieties are chemically bonded to organic polymeric matrix and uniformly distributed within the system, thereby enhancing the thermal and mechanical properties of the resultant hybrid materials.[5,16,30–33]

In our lab, we have made considerable efforts toward the preparation of POSS-containing nanocomposites, and our attention has especially focused on their T_g reinforcement mechanism. With monofunctional POSS monomers and alkene monomers, we have synthesized several linear-type (or pendant-type) hybrid nanocomposites such as poly(acetoxystyene-*co*-isobutyl POSS) (PAS-POSS),[34,35] poly(vinyl pyrrolidone-*co*-isobutyl POSS) (PVP-POSS)[36] and poly(hydroxyvinylpyrrolidone-*co*-vinylpyrrolidone-*co*-isobutyl POSS) (PHS-PVP-POSS).[37] We found that resulting T_g of the nanocomposites is related to the content of the incorporated POSS molecules and the existence of specific interactions (especially the hydrogen bonding) within the hybrid polymeric matrix and subsequently leads to T_g change. Generally, at very low POSS content, T_g of the nanocomposite decreases without hydrogen bonding formation where the presence of POSS plays a diluent role reducing the self-interaction of parent polymer. However, at relatively high POSS contents, even

Correspondence to: H. Xu (hongyaoxu@163.com).
Contract grant sponsor: National Natural Science Fund of China; contract grant numbers: 90606011, 50472038.
Contract grant sponsor: Program for New Century Excellent Talents in University of China; contract grant number: NCET-04-0588.
Contract grant sponsor: Ph.D. Program Foundation of Ministry of Education of China; contract grant number: 20070255012.

without the hydrogen bonding, the dipole–dipole interactions between POSS and polar groups (e.g., carbonyl) of the parent polymers play a dominant role and result in T_g increase.

Recently, we have turned our attention toward the preparation of star or crosslinked POSS-containing nanocomposites based on multifunctional POSS monomers to explore the effect of POSS and parent polymer structures on the thermal properties of resulting hybrid nanocomposites. We report the syntheses and characterization of crosslinking PVP-POSS hybrid nanocomposites from vinyl pyrrolidone and octavinyl-polyhedral oligomeric silsesquioxane using free radical polymerization technique. The thermal properties of the nanocomposites are investigated by DSC and TGA and the T_g increase mechanism is discussed in detail.

EXPERIMENTAL

Materials

N-vinylpyrrolidone (98%) was purchased from Aldrich, distilled from calcium hydride under reduced pressure and stored in sealed ampoules in a refrigerator prior to use. Azobis(isobutyronitrile) (AIBN) was obtained from Shanghai Reagent Co. and refined in heated ethanol and stored in a dried box. Spectroscopic-grade THF and 1,4-dioxane were dried over 4-Å molecular sieves and distilled from sodium benzophenone ketyl immediately prior to use. All other reagents were used without further purification.

Syntheses of octavinyl-POSS

The octavinyl-polyhedral oligomeric silsesquioxane (OV-POSS) was synthesized according to a previous report.[38] Typically, vinyltriethoxysilane (10.5 mL, 0.05 mol) was dissolved in 24.5 mL of anhydrous ethanol with stirring and then some amount of hydrochloric acid and 3 mL of water were added to adjust solution to pH 3. The system was allowed to react for 10 h at 60°C under N_2, and the resulted mixture was cooled to room temperature. The white crystalline powder was filtered, washed with cyclohexane and recrystallized from tetrahydrofuran/methanol (1 : 3) to give 0.72 g (18.2%).

FTIR (KBr, ν, cm^{-1}): 1605(CH=CH), 1414, 1273(C—H), 1109(Si—O—Si);

^{1}H-NMR: ($CDCl_3$, ppm) 5.58 (HHC=CH^b, 8H, dd, J = 12.4 and J = 15.0 Hz), 6.01(HH^a'C=CH, 8H, dd, J = 2.4 and J = 12.4 Hz), 6.10 (H$^a H^a$'C=CH, 8H, dd, J = 2.4 and J = 15.0 Hz).

Syntheses of PVP-POSS nanocomposites

Polymerization was carried out using a standard Schlenk vacuum-line system under a nitrogen atmosphere. For comparison, the polyvinylpyrrolidone (PVP) homopolymer was also synthesized. In a typical reaction, 0.14 mmol of OV-POSS and 9.37 mmol of *N*-vinylpyrrolidone in 5 mL of 1,4-dioxane were added in a three-necked flask, stirred for 12 h at 80°C, using the AIBN initiator (1 wt % on the basis of monomer). The crude product was added dropwise into excessive ethanol at 60°C under vigorous agitation to dissolve any unreacted monomers and precipitate the nanocomposite. The precipitated product was further purified by Soxhlet extraction method using ethanol as the solvent for 24 h to ensure thorough removal of the OV-POSS and *N*-vinylpyrrolidone from the PVP-POSS nanocomposite. Finally, the purified product was dried in a vacuum oven at 30°C for 4 h. A yield of 58 wt % was obtained through this procedure.

Measurement and techniques

The FTIR spectra were measured with a spectral resolution of 1 cm^{-1} on a Nicolet NEXUS 870 FTIR spectrophotometer using KBr powder at room temperature. ^{1}H-NMR spectra were recorded on a Bruker AVANCE/DMX 300 spectrometer using chloroform-*d* solvent. High-resolution ^{29}Si-NMR spectra were carried out at room temperature using a Bruker DSX-400 spectrometer operating at resonance frequency of 79.49 MHz. Weight-average (M_w), number-average (M_n) molecular weights, and polydispersity index (PDI, M_w/M_n) were determined by a Waters 515 gel permeation chromatograph (GPC). Differential scanning calorimetry (DSC) was performed on a TA Instruments DSC 9000 under a continuous nitrogen purge (50 mL/min). The scan rate was 20°C/min at a temperature range of 20–50°C. The glass-transition temperature (T_g) was taken as the midpoint of the specific heat increment. Thermogravimetric analyses were carried out using a TA Instruments TGA 2050 thermogravimetric analyzer with a heating rate of 10°C/min from 25 to 550°C under a continuous nitrogen purge (100 mL/min). The thermal degradation temperature (T_{dec}) was defined as the temperature of 5% weight lost.

HF-treated samples for GPC analysis

The organic chains connected on or between POSS cages were prepared by dissolving the silica core (POSS) with hydrofluoric acid (HF) and extracted for GPC analyses. In a typical procedure, 0.05 g of the PVP-POSS nanocomposite was dissolved in 5 mL of THF in a polytetrafluoroethylene bottle. 0.05 mL of

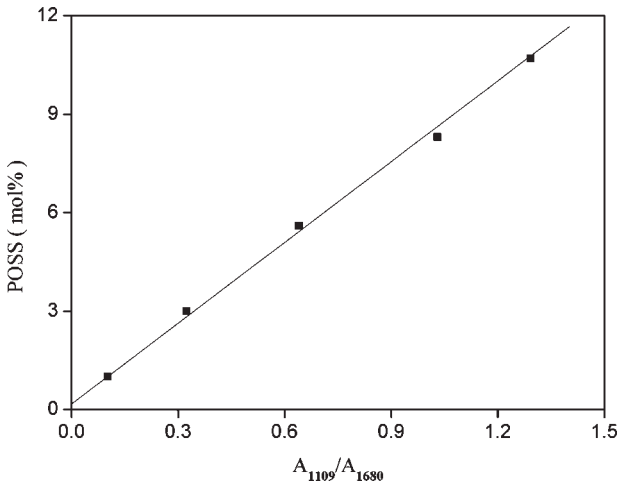

Figure 1 IR calibration curve for determining POSS contents in PVP-POSS hybrid Nanocomposites.

50% HF was dropped into the solution, and the mixture was kept at room temperature for 72 h. Then, THF was removed by rotary evaporation. The residual material was mixed with freshly dried ether to extract the organic components. The extracted solution was filtered and ether in the filtrate solution was removed. A viscous liquid was obtained and dissolved in 1 mL of THF for GPC analysis.

POSS content determination

The POSS content in the PVP-POSS nanocomposite was determined by the FTIR technology. On the IR spectra, PVP has a characteristic absorption band at 1680 cm^{-1} (carbonyl) whereas the POSS shows no absorption in this region. The POSS shows an absorption band at $\sim$ 1109 cm^{-1} while PVP does not display any absorption in this region. As a result, the POSS content in the PVP-POSS nanocomposite can be estimated by the calibration curve method (Formula 1). A series of PVP/POSS mixtures with different POSS contents were first dissolved in THF to ensure even mixing and then cast into thin films for FTIR determination. The calibration curve of A_{1109}/A_{1680} against POSS molar contents in the mixtures was plotted shown in Figure 1. The linear relationship between POSS molar percentage (Y_{POSS}) and A_{1109}/A_{1680} is expressed as Formula 1.

$$Y_{POSS} = 0.082(A_{1109}/A_{1680}) - 0.0019 \quad (1)$$

RESULTS AND DISCUSSION

Structure characterization of nanocomposites

The PVP-POSS nanocomposites prepared by free radical polymerization techniques are shown in Scheme 1. For comparison, the polyvinylpyrrolidone homopolymer (PVP) was also synthesized. Figure 2 shows the FTIR spectra of pure POSS, PVP, and PVP-POSS. The pure POSS shows a characteristic Si—O—Si stretching absorption band at $\sim$ 1109 cm^{-1}. The pure PVP shows two characteristic absorption bands at 1680 and 1284 cm^{-1}, which are assigned to carbonyl and C—N stretching, respectively. The stretching absorption bands of methylene and methine groups are located at $\sim$ 2900 cm^{-1}. The

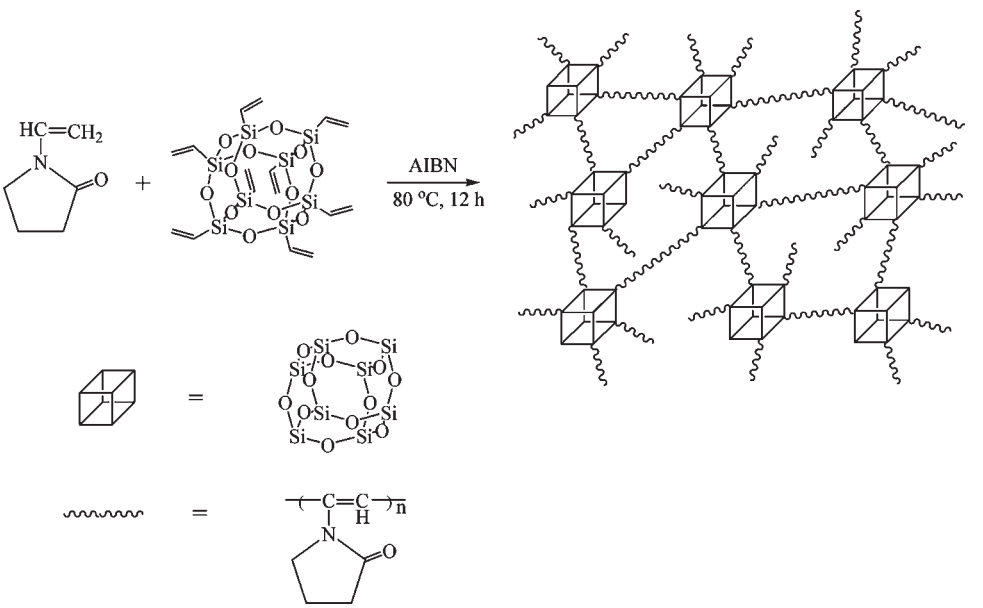

Scheme 1 Formation of PVP-POSS nanocomposites via free radical polymerization.

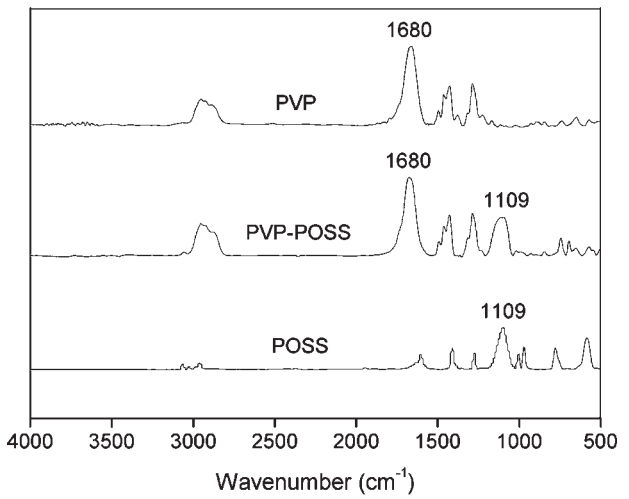

Figure 2 The FTIR spectra of pure POSS, PVP, and PVP-POSS Nanocomposites.

spectra of all PVP-POSS nanocomposites are similar to that of the PVP except that a strong and symmetric peak appears at $\sim$ 1109 cm^{-1} in all the spectra, a characteristic Si—O—Si stretching of the silsesquioxane cage. In addition, the intensity of this vibration absorption increases with the increase of the POSS feed ratio, implying that the POSS cage is indeed incorporated into the polymeric matrix.

By detecting the A_{1109}/A_{1680} values of the PVP-POSS nanocomposites, the POSS molar contents in the hybrid nanocomposites were determined on the basis of the calibration curve (Fig. 1), and the results are shown in Table I. Table I indicates that the molar content of the POSS in the nanocomposites increases with the increase of POSS feed ratio, showing that the content of POSS in the nanocomposites can be effectively adjusted by varying POSS feed ratio.

Figure 3 shows ^{1}H-NMR spectra of POSS, PVP, and PVP-POSS (Table I. No 2) in *d*-chloroform solvent. For the pure POSS macromer, the resonance band of vinyl protons is located at $\sim$ 6.0 ppm as multiple peaks because of the coupling of hydrogen protons. For PVP homopolymer, the broad resonance bands at 3.7 ppm and 3.2 ppm are respectively, attributed to the methine proton connected to pyrrole ring and the methylene proton just next to nitrogen element on the pyrrole ring. Two broad bands around 2.2 and 2.0 ppm correspond to other two methylene protons on the pyrrole ring. The peak at 1.5 ppm is assigned to the methylene proton in the polymeric chain. The PVP-POSS shows a similar spectrum to that of the pure PVP except that these bands ranging from 1.0 to 2.5 ppm become broadened due to the band overlapping between VP and POSS moieties. Besides, there is a wide and weak resonance band near 6 ppm from the unreacted vinyl protons of POSS molecules.

The high-resolution solid-state ^{29}Si-NMR spectroscopy provides further insight to the copolymerization of vinylpyrrolidone with POSS macromer. Figure 4 shows the ^{29}Si-NMR spectra of both pure POSS macromer and PVP-POSS nanocomposite (7.54 mol % POSS). The pure octavinyl-POSS gives only one resonance peak at -79.5 ppm since essentially all silicon atoms have the same chemical environment in the POSS molecule. The nanocomposite shows two resonance bands at -65.5 and -79.0 ppm, corresponding to silicon atoms connected to the reacted and unreacted vinyl groups on the POSS cage. Because the peak area at -65.5 ppm is substantially larger than that at -79.0 ppm, we speculate that most vinyl groups of each POSS molecule have participated in the copolymerization with vinylpyrrolidone to form hybrid nanocomposites. By calculating the peak area ratio, we estimate that about 5.7 vinyl groups on each POSS cage have been consumed in the copolymerization reaction. This result implies that the resulting hybrid nanocomposites are possibly of star-shaped or network structures.

To further study the structure of the nanocomposites, we tested the solubility of these resultant nanocomposites in a number of solvents such as $CHCl_3$, THF, dioxane and so on. These nanocomposites can

TABLE I
Effect of POSS Feed Ratio on the Properties of PVP–POSS Nanocomposites

No	POSS (mol %) Feed mole ratio	POSS (mol %) Product mole ratio[a]	Yield (wt %)	M_w[b] ($\times 10^3$ g/mol)	M_n ($\times 10^3$ g/mol)	PDI	T_g[c]	T_{dec}[d]	Char yield (%)
1	0.00	0.00	60.5	158	115	1.38	144.2	415.3	12.8
2	1.50	2.78	58.1	138	113	1.22	150.2	416.8	17.7
3	2.25	3.91	55.7	–	–	–	155.6	419.8	24.7
4	4.83	6.33	50.4	–	–	–	164.2	421.4	31.6
5	5.83	7.54	44.2	–	–	–	–	431.8	32.5

[a] Data were obtained based on the IR standard curve.
[b] Data were determined by GPC using the PS standard curve.
[c] Data were gathered on the second melt using a heating rate of 10°C/min.
[d] Data were taken to be the temperature at 5% weight loss.

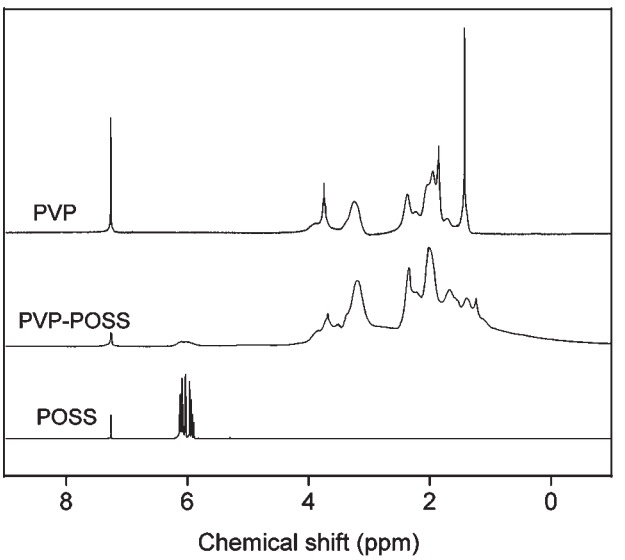

Figure 3 The ^{1}H-NMR spectra of pure POSS, PVP, and PVP-POSS with POSS content 2.78% (Table I. No. 2).

be dissolved in most common solvents when the POSS content is less than 3.0 mol %, implying that these resultant nanocomposites may possess star or low crosslinking structure. When the POSS content is greater than 3.0 mol %, all nanocomposites are insoluble in any solvents, indicating that they may be as network structures. To support our presumption, we filtered all the as-synthesized solutions with a 0.22 μm membrane and the filtered solutions were analyzed by GPC and FTIR. We found that when POSS content is less than 3.0 mol %, GPC and FTIR give normal response as shown in Table I and Figure 2. When the POSS content is more than 3.0 mol %, both GPC and FTIR do not display response of polymers or give very weak information of polymer, implying that almost no polymeric substance passes through the membrane filter during filtration. This observation provides further evidence that these products are crosslinking gels with network structures because the poly(vinylpyrrolidone-*co*-styrenyl-POSS)[35] with pendant POSS is completely soluble in common solvent. The result also hints that the solubility of result hybrid nanocomposites may be adjusted by varying POSS feed ratio. This result is also different from our previous study on PAS-POSS[39] and PS-POSS,[40] which are either star or low crosslinking structure and thus are soluble in common solvents. We contribute this difference to the reactivity difference between polymeric propagating radicals. To further study the polymer structure, we treated our products with HF to dissolve the POSS cores and leave behind PVP chains, and then used GPC to determine the molecular weight distribution of the PVP chains. We found that, for product No 2, the molecular weight of most PVP chains were around 5000–7000, and only $\sim$ 20% of the chains were about 10,000–12,000 in molecular weight. It may indicates that most of the PVP chains were the side chains of the POSS cages, and only small amount of them were the linking chains between POSS cages. On the basis of the calculation of the POSS contents in PVP-POSS copolymers, we found that when POSS content was low (less than 3.0 mol %), there were only 3–4 POSS molecules in one PVP-POSS polymer, indicating that these PVP-POSS copolymers may have linear or low crosslinking structure, accounting for its good solubility. When POSS content was higher (more than 3.0 mol %), PVP chains with relative lower molecular weight take higher proportion, showing that PVP-POSS copolymers may have higher degree of crosslinkage, indicating that the degree of crosslinkage can be adjusted by varying the feed ratio of POSS.

Thermal properties and T_g improvement mechanism

Figure 5 shows the DSC thermograms of PVP-POSS hybrid nanocomposites with various POSS contents. For comparison, PVP homopolymer thermogram is also displayed. As is seen, T_g's of all PVP-POSS nanocomposites are higher than that of PVP homopolymer. The T_g of the nanocomposite increases gradually with the increase of the POSS contents. For example, the T_g of PVP-POSS with 2.78 mol % of POSS (PVP-POSS2.78) at 150.2°C is higher than 144.2°C of the PVP homopolymer. When the molar content of POSS in the nanocomposite is increased to 6.33 mol %, the glass-transition temperature

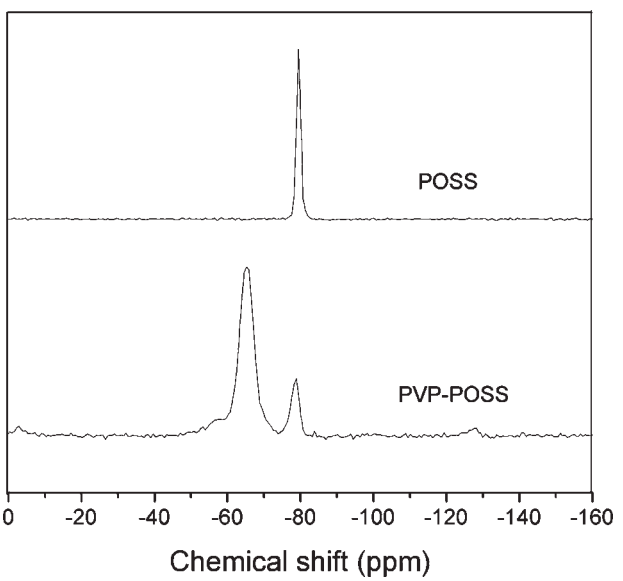

Figure 4 High-resolution solid-state ^{29}Si-NMR spectra of pure POSS and PVP-POSS with POSS content 2.78% (Table I. No. 5).

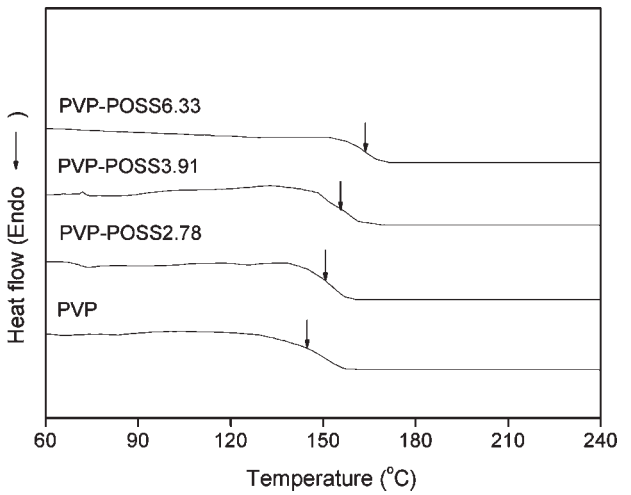

Figure 5 The DSC thermograms of pure PVP and PVP-POSS nanocomposites.

reaches as high as 164.2°C, which is 20.0°C higher than the T_g of the PVP homopolymer.

The synthesized POSS-containing naocomposites were characterized by network structures. Within these naocomposites, POSS cores act as joint points which restrict the free motion of PVP chains, leading to the T_g enhancement. More POSS cores mean more joint points, resulting in higher T_g. When the POSS content is too high (in our case, higher than 7.0 mol %), no T_g can be detected because the high crosslinkage completely restricts the movement of PVP chains.

In view of our previous study,[35] we think that the dipole–dipole interaction between PVP chains and POSS cores may be another important factor to affect the T_g. To investigate the contribution of dipole–dipole interaction to T_g reinforcement, the FTIR characterization of PVP-POSS nanocomposites was carried out. Figure 6 shows the expanded FTIR spectra of pure PVP and various PVP-POSS nanocomposites ranging from 1720 to 1620 cm^{-1}. The pure PVP shows the characteristic carbonyl absorption at 1665 cm^{-1}. When the POSS is incorporated into the PVP, the carbonyl absorption begins to shift to higher wavenumber. For example, when 2.78 mol % POSS is incorporated into the PVP (PVP-POSS2.78), the carbonyl absorption shifts to 1669 cm^{-1}. There is a trend that the carbonyl absorption peak shifts toward higher wavenumber with the increase of POSS content, indicating the increase of dipole–dipole interactions between PVP and POSS in these nanocomposites. Apparently, this dipole–dipole interaction, in addition to the contribution of crosslinking, will further limit the PVP chain movement and yields positive contribution to the T_g increase of the nanocomposite.

Figure 7 shows the TGA thermograms of various PVP-POSS hybrid nanocomposites and pure PVP. The temperatures of 5% weight loss (T_{dec}) and the char yield are recorded in Table I. The PVP homopolyer has a T_{dec} at 415.3°C, and has 12.8% remnant when the temperature reaches 600°C under N_2. For PVP-POSS nanocomposites, their T_{dec} and char yields increase with the increase of POSS contents. For example, PVP-POSS2.78 (POSS content is 2.78 mol %.) has a T_{dec} at 416.8°C, 1.5°C higher than the pure PVP, and 17.7% char yield at 600°C. Although PVP-POSS7.54 has a T_{dec} at 431.8°C, 16.5°C higher than pure PVP, and 32.5% char yield at 600°C. This fact confirms that the incorporation of POSS into polymeric matrix is possible to improve the thermal stability of polymeric materials.

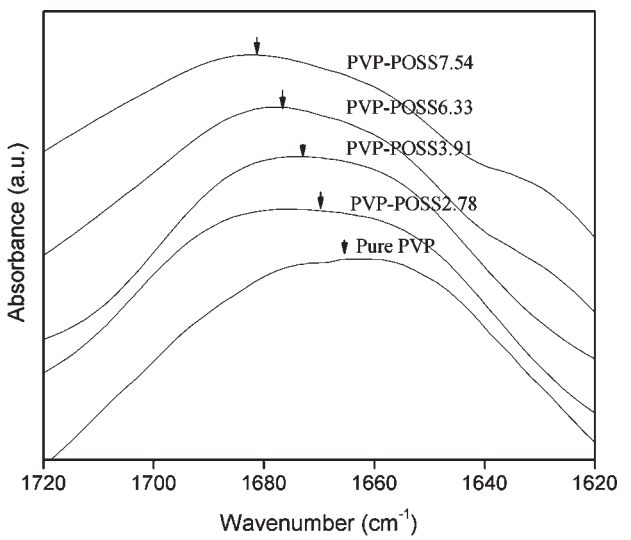

Figure 6 The expanded FTIR spectra in the region from 1720 cm^{-1} to 1620 cm^{-1} of pure PVP and PVP-POSS nanocomposites.

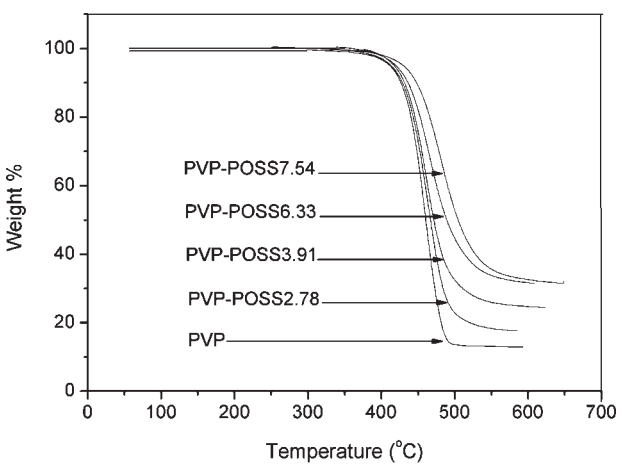

Figure 7 The TGA thermograms of pure PVP and PVP-POSS Nanocomposites.

CONCLUSIONS

The well-defined nanosize polyhedral oligomeric silsesquioxane (POSS) is incorporated into the polyvinylpyrrolidone by common free radical polymerization to form PVP-POSS hybrid nanocomposites. The structures of the PVP-POSS hybrid nanocomposites characterized by FTIR, ^{1}H-NMR, and ^{29}Si-NMR indicate that these resultant nanocomposites are of network structures and the degree of crosslinking is affected by POSS content, which increases with the increase of the POSS content in the composites. Thus, the solubility and molecular structure of resultant hybrid nanocomposites was controlled by varying POSS feed ratio. Thermal properties of these PVP-POSS hybrid nanocomposites were studied by the DSC and TGA techniques. Both glass transition temperature and decomposition temperature of the nanocomposite increase with the POSS content. The remarkable increase of the thermal properties is primarily due to the network structure of the nanocomposites and the dipole–dipole interaction between POSS cores and PVP carbonyl groups.

References

1. Haddad, T. S.; Lichtenhan, J. D. Macromolecules 1996, 29, 7302.
2. Lichtenhan, J. D.; Otonari, Y. A.; Carri, M. J. Macromolecules 1995, 28, 8435.
3. Pyun, J.; Matyjaszewski, K. Macromolecules 2000, 33, 217.
4. Mather, P. T.; Jeon, H. G.; Romo-Uribe, A.; Haddad, T. S.; Lichtenhan, J. D. Macromolecules 1999, 32, 1194.
5. Li, G. Z.; Cho, H. S.; Wang, L. C.; Toghiani, H.; Pittman, C. U., Jr. J Polym Sci Part A: Polym Chem 2005, 43, 355.
6. Zheng, L.; Farris, R. J.; Coughlin, E. B. Macromolecules 2001, 34, 8034.
7. Coughlin, E. B.; Farris, R. J.; Zheng, L. J Polym Sci Part A: Polym Chem 2001, 39, 2920.
8. Lee, A.; Lichtenhan, J. D. Macromolecules 1998, 31, 4970.
9. Coughlin, E. B.; Farris, R. J.; Zheng, L. Polym Prepr (Am Chem Soc, Div Polym Chem) 2001, 42, 885.
10. Fu, B. X.; Zhang, W.; Hsiao, B. S.; Johansson, G.; Sauer, B. B.; Phillips, S.; Balnski, R.; Rafailovich, M.; Sokolov, J. Polym Prepr 2000, 41, 587.
11. Fu, B. X.; Hsiao, B. S.; Pagola, S.; Stephens, P.; White, H.; Rafailovich, M.; Sokolov, J.; Mather, P. T.; Jeon, H. G.; Phillips, S.; Lichtenhan, J.; Schwab, J. Polymer 2001, 42, 599.
12. Costa, R. O. R.; Vasconcelos, W. L.; Tamaki, R.; Laine, R. M. Macromolecules 2001, 34, 5398.
13. Muthukrishnan, S.; Plamper, F.; Mori, H.; Muller, A. H. E. Macromolecules 2005, 38, 10631.
14. Huang, J. C.; Li, X.; Lin, T.; He, C. B.; Mya, K. Y.; Xiao, Y.; Li, J. J Polym Sci Part B: Polym Phys 2004, 42, 1173.
15. Xiong, S. X.; Xiao, Y.; Ma, J.; Zhang, L. Y.; Lu, X. H. Macromol Rapid Commun 2007, 28, 281.
16. Liang, K. W.; Toghlani, H.; Li, G. Z.; Pittman, C. U., Jr. J Polym Sci Part A: Polym Chem 2005, 43, 3887.
17. Mayadunne, R. T. A.; Jeffery, J.; Moad, G.; Rizzardo, E. Macromolecules 2003, 5, 1505.
18. Zheng, G. H.; Pan C. Y. Polymer 2005, 8, 2802.
19. Deng, G.; Chen, Y. Macromolecules 2004, 1, 18.
20. Zhao, Y. L.; Chen, Y. M.; Chen, C. F.; Xi, F. Polymer 2005, 15, 5808.
21. Huang, C. F.; Lee, H. F.; Kuo, S. W.; Xu, H. Y.; Chang, F. C. Polymer 2004, 7, 2261.
22. Liu, Y. H.; Meng, F. L.; Zheng, S. X. Macromol Rapid Commun 2005, 26, 920.
23. Liu, H. Z.; Zheng, S. X. Macromol Rapid Commun 2005, 26, 196.
24. Liu, Y. L.; Chang, G. P.; Hsu, K. Y.; Chang, F. C. J Polym Sci Part A: Polym Chem 2006, 44, 3825.
25. Liu, Y. L.; Chang, G. P. J Polym Sci Part A: Polym Chem 2006, 44, 1869.
26. Chen, Q.; Xu, R. W.; Zhang, J.; Yu, D. S. Macromol Rapid Commun 2005, 26, 1878.
27. Fasce, D. P.; Williams, R. J. J.; Balsells, R. E.; Ishikawa, Y.; Nonami, H. Macromolecules 2001, 34, 3534.
28. Tamaki, R.; Tanaka, Y.; Asuncion, M. Z.; Choi, J.; Laine, R. M. J Am Chem Sci 2001, 123, 12416.
29. Ni, Y.; Zheng, S. X. Macromol Chem Phys 2005, 206, 2075.
30. Isayeva, I. S.; Kennedy, J. P. J Polym Sci Part A: Polym Chem 2004, 42, 4337.
31. Gunji, T.; Iizuka, Y.; Arimitsu, K.; Abe, Y. J Polym Sci Part A: Polym Chem 2004, 42, 3676.
32. Wahab, M. A.; Kim, I.; Ha, C. S. J Polym Sci Part A: Polym Chem 2004, 42, 5189.
33. Liu, Y. L.; Chang, G. P.; Wu, C. S.; Chiu, Y. S. J Polym Sci Part A: Polym Chem 2005, 43, 5787.
34. Xu, H. Y.; Kuo, S. W.; Huang, C. F.; Chang, F. C. J Polym Res 2002, 9, 239.
35. Xu, H. Y.; Kuo, S. W.; Lee, J. S.; Chang, F. C. Macromolecules 2002, 35, 8788.
36. Xu, H. Y.; Kuo, S. W.; Huang, C. F.; Chang, F. C. J Appl Polym Sci 2004, 91, 2208.
37. Xu, H. Y.; Kuo, S. W.; Lee, J. S.; Chang, F. C. Polymer 2002, 43, 5117.
38. Harrison, P. G.; Hall, C.; Kannengiesser, R. Main Group Met Chem 1997, 20, 515.
39. Xu, H. Y.; Yang, B. H.; Wang, J. F.; Guang, S. Y.; Li, C. Macromolecules 2005, 38, 10455.
40. Yang, B. H.; Xu, H. Y.; Wang, J. F.; Guang, S. Y.; Li, C. J Appl Polym Sci 2007, 106, 320.